Development of a Desktop Freehand 3-D Surface Reconstruction System

K. C. Lim, M. Boissenin, B.P. Amavasai, R. Saatchi

***Abstract*—This paper discusses the development of a freehand 3-D surface reconstruction system. The system was constructed by making use of readily available off-the-shelf components, namely a laser line emitter and a webcam. The 3-D laser scanner system allows the user to hand sweep the laser line across the object to be scanned. The 3-D surface information of the object is captured as follows. A series of digital images of the laser line, generated by the intersection of the laser plane, the surface of the object and the background planar object were captured and stored in a PC. The points on the laser line were extracted. The 2-D laser points that were found on the surface of the planar object were projected onto the 3-D space using a pinhole camera model. The laser plane was calibrated. Using the 2-D laser points found on the surface of the 3-D object, a cloud of 3-D points which represent the surface of the object being scanned was generated by triangulation. For the laser plane calibration two different methods were implemented. Their performance were compared.**

***Index Terms*—Freehand, 3-D surface reconstruction, planar homography, laser plane self-calibration.**

I. Introduction

Due to the increase in computing power of personal computers and the availability of inexpensive high resolution webcams it has now become possible to develop a desktop-based 3-D surface reconstruction systems. 3-D surface reconstruction systems can be implemented either by adapting stereo vision based approaches[1], using two calibrated cameras, or by adapting optical triangular based approaches using a calibrated camera and an external optical device such as a laser line emitter. However, the stereo vision based techniques suffer from the correspondence problem when patches of uniform colours cannot be correlated accurately, resulting in imprecise geometric information of these regions[23]. Moreover, the precision of stereo vision methods are inversely proportional to the distance of the object to the cameras.

To move the camera and the laser plane emitter around the scanning object, traditional non-stereo optical based 3-D reconstruction systems make use of different mechanical systems, like linear translator[2], scanning rig[3], or articulated arm[4]. The mechanical system can also be a turntable to rotate the object itself[5][6]. The images of the deformed laser line, formed by the intersection of the laser plane and the scanned object, are captured using a camera. The points on the laser line are extracted and will then be triangulated to produce a cloud of 3-D points. These cloud of points represent the surface of the scanned object. For other non-stereo optical based systems, where the position of the camera has to remain static throughout the scanning process, *e.g.* structured light based methods[1][6][7], several scans are required from different camera view points of the scanned object. The resulting clouds of 3-D points, from different camera view points, are then registered in software using correspondence matching of the acquired 3-D points[8].

One of the advantages of freehand scanning is that the user may repeatedly scan the same surface of interest, to generate more 3-D points to represent the surface and hence increase the signal to noise ratio by "brushing" across the surface a few times. For the triangulation process one needs to know the pose of the laser plane. To obtain the pose of the laser plane, the laser line emitter could be attached to a mechanical articulated arm, or wireless sensors or light reflecting markers which could be tracked, can be attached to the laser line emitter and hence provides the pose of the laser plane. These methods for estimating the pose of the laser plane have limitations. For example the articulated arm might limit the movement of the operator, due to the extra weight of the attached position sensor or the markers could get occluded and might disturb the scanning process. Other novel ways had been proposed to estimate the pose of the laser plane, by using reference planes[1][8] and reference frame[9]. In this paper, to estimate the pose of the laser plane, we have adopted the reference plane method proposed by Bouguet in [1] and Winkelbach in [8]. Rest of this paper will discuss the overall architecture and the design of the 3-D laser scanning system. The paper is structured as follows: in section 2 we will describe the software and the hardware components of the system and in Section 3 the results of the 3-D surface scanning performed using the 3-D laser scanner will be discussed.

II. Implementation

In this section we shall discuss in detail the hardware and the software implementation of the laser scanning system.

A. Hardware Implementation

A digital camera, two planar objects and a laser line generator are the three major components of the 3-D scanning system. The digital camera used was capable of resolutions of up to 640x480 pixels frame size. It was connected to a personal computer through a USB interface. The camera's intrinsic parameters can either be estimated using a 2-D planar object[16], which is implemented by Bouguet [10], or using the method provided in the Mimas toolkit[22]. In our implementation we used the one by Bouguet [10]. The laser

Manuscript received May 23, 2008.

K. C. Lim is doing his PhD at the Sheffield Hallam University, Sheffield, S1 1WB UK (phone: +44(0)1142253301; e-mail: lim.kim.chuan@gmail.com).
The author was supported by the scholarship body at University Teknikal Malaysia Melaka (UTeM).

line generator used was a class 2 laser line emitter with 20mW power and 690nm wavelength. Two planar objects with checker board patterns were placed in an arrangement as shown in figure 1. Unlike what was proposed in [1] and [8], the angle between the planes need neither be ninety degrees nor be known.

B.Software Implementation

An overview of the operation of the freehand laser scanning system is provided below. First a stationary calibrated camera was placed in such a way as to be able to view the object to be scanned and the two planar reference objects. The image of the planar objects with the checker board pattern on it was captured and stored. This image shall be referred to as the background image (Img_{bg}). Using Img_{bg} of the planar object, the pose of the two planes, the horizontal plane(${}^{C}T_{H}$) and the vertical plane(${}^{C}T_{V}$) with respect to the camera frame as global reference frame were estimated (Figure 2). In the scene image a region of interest was then defined to enclose the object to be scanned. Using a laser line emitter a laser line was swept across the surface of the object. To use the principle of triangulation, the angle in between the viewing axis of camera and laser plane should be as large as possible. The images (Img_{L}) of the laser line sweeping across the object were captured. The points on the laser line seen in the image were generated by the laser plane intersecting the horizontal and the vertical plane of the planar object and the surface of the object being scanned. These points were detected and their 2-D co-ordinates were estimated in each of the images. Knowing the pose of the planes, of the planar object, the laser points laying on the two planes were transformed to their corresponding 3-D coordinate points, with respect to the camera coordinate system. By making use of this estimated 3-D coordinates, of the points on the laser plane, the equation representing the laser plane in each of the images was estimated. Knowing the equation of the laser plane, in each of the images, the 3-D coordinates of all the laser points on the surface of the object were estimated for each of the images. These points represent the points on the surface of the object, that was being scanned. A cloud of 3-D points representing the surface of the object being scanned was thus created at the end of the scanning process. Powercrust [12], an open source algorithm for 3-D surface reconstruction was applied to the cloud of 3-D points to create a set of polygon mesh and thus to approximate the surface of the reconstructed object. MeshLab[13], an interactive, open source 3-D viewing and mesh editing program, was then used to display and smooth the generated set of polygon mesh.

The software for the laser scanner system had been implemented and integrated into our vision toolkit, Mimas[14]. Mimas is an open source C++ computer vision software toolkit, with an emphasis on real-time applications. To implement the graphical user interface, Qt [15], an open source cross-platform developing toolkit, was used. The theoretical background for the above discussed implementation of the free-hand laser scanner system will be discussed in detail in the following sections.

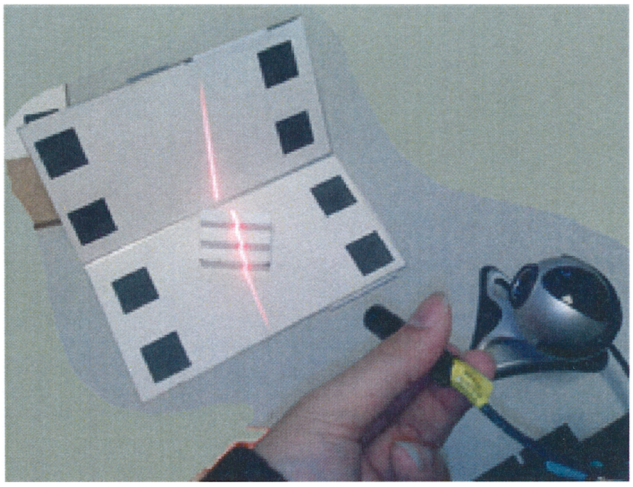

Figure 1: The planar object and the object to be scanned placed at the center of the horizontal plane.

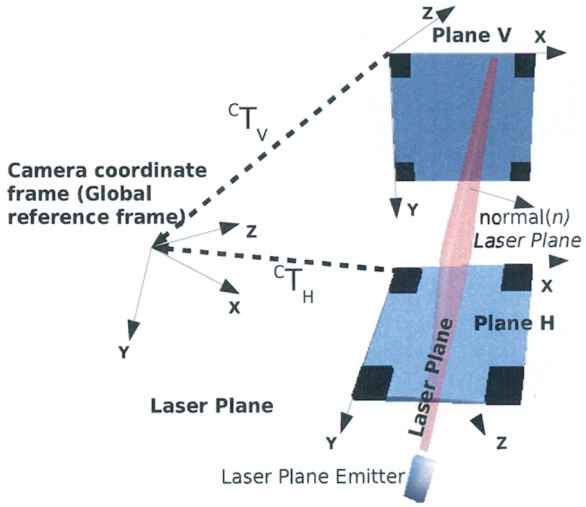

Figure 2: System coordinate frames and notation.

1) Background plane, planar homography and pose estimation

Plane pose estimation was used to estimate a 4x4 transformation matrix which represents the rotation and the translation of the plane with respect to a reference coordinate system. The planar object with a checker board pattern was considered as an XY plane. The top left hand corner of the pattern, in each of the planes, was taken as the origin and the normal to the plane was taken as the Z-axis of the 3-D coordinate system (using right hand rule system). Using Zhang's[16] proposed planar homography method, the planar homography ($H_{\{V,H\}3x3}$) for both the background planes were estimated. This was done by detecting the corners of the checker board patterns and making use of the corresponding grid coordinates (Figure 3) of the patterns. Using the calibrated camera's intrinsic parameters the poses of two background planes were extracted from the estimated planar homographies[16].

Equation (1) can be used to resolve the angle between the two detected planes. The Estimated angle between the planes

can be used to verify the accuracy of the camera calibration, assuming that the pose estimation of the planes was relatively accurate.

$$\theta_{plane}=\cos^{-1}(\vec{n}_{P_H}\cdot\vec{n}_{P_V})*180/\pi \quad (1)$$

Where

$$\vec{n}_{P_i}={}^{C}T_{i_3}$$

is a 3-D vector which is the 3rd column of the estimated plane pose 4x4 matrix.

One can also make use of a preexisting structure, as two planes orthogonal to each other, to perform the test of accuracy of the camera intrinsics parameters, where the value of θ_{plane} should be approximately ninety degrees. For example the checker board pattern can be placed in the corner of a room as suggested in [8]. The Euclidean distance, d_{HV}, between the origin of the two planes can then be estimated using (2). Knowing the actual distance, the accuracy of the camera intrinsic parameters can be evaluated.

$$d_{HV}=P_{H_4}-P_{V_4} \quad (2)$$

Where

$$P_{i_4}={}^{C}T_{i_4}$$

is a 3-D vector which is the 4th column of the estimated plane pose 4x4 matrix.

2)Laser points detection.

Making use of the colour characteristics of the pixels illuminated by the laser, the image location of the points on the laser line were found. By knowing the typical RGB (Red, Green Blue colour space) or HSV (Hue, Saturation, Value colour space) values of the points, illuminated by the laser, one can detect and isolate those points in the image. The method will work best in a controlled environment where conditions like ambient light can be controlled. For example if the ambient light is completely eliminated only a partial power of the laser light need to be used. Because on full power, the laser light is likely to be scattered. Also in a controlled environment one can make use of known values of RGB or HSV to threshold the points illuminated by the laser. Through experimentation it was found that using HSV threshold range gave better results, in isolating image locations illuminated by the laser line, than the corresponding RGB values. Hence HSV threshold values were used to filter the image to isolate the laser points.

If one does not have a control on the environment like lighting condition, an inappropriate threshold value will result in the false detection of laser points. Hence instead of using threshold values, a better way of detecting the laser points was designed and is explained herein. Two images of the scene were captured. The first one is the image of the background (Img_{bg}) without the laser line and the second image is that of the scene with the laser line (Img_L). The normalized image (Img_{norm}), between the values 0 to 255, of the difference between the two images Img_L and Img_{bg}, will give an approximation of the location of the laser points. The laser points were identified by thresholding the normalized image (Img_{norm}) using a value around 255. Blais and Rioux fourth order sub pixel estimator[17] was subsequently used to estimate the coordinates of the laser points to sub-pixel accuracy. This estimation process resulted in a single laser point location for each row of the image. Care should be taken that the laser line intersects both the planar planes.

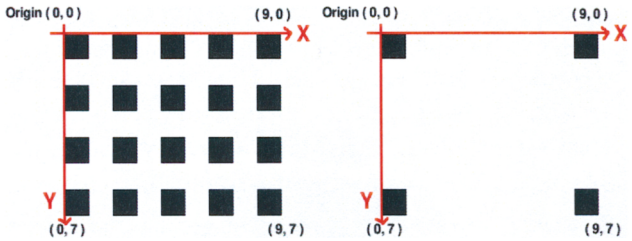

Figure 3: Grid coordinate system for each corners of the planar checker board pattern(left). The intermediate black squares have been removed(right) to provide a better laser point detection

3)Laser plane pose estimation

Two different methods were explored to estimate the equation of the laser plane. In the first method the fact that the laser line is formed by the intersection of the laser plane with the planar object, was used. In the second method the laser plane equation was estimated, in 3-D space, by fitting the best fitting plane to all the points detected to be lying on the laser line. The above two methods, of estimating the laser plane equation, are described in detail below.

For the first method, to define the equation of a plane, a minimum of three non co-linear points are needed. Hence the points that are lying on the laser plane need to be found first. This was done by detecting the points lying on the laser line, as described in the section B.2. The laser points which fall within the vertical plane, of the background planar object, were separated from those falling within the horizontal plane of the planar background object. Using the Hough transform (HT)[18] two 2-D lines, one from the horizontal plane and one from vertical plane, were detected. Two points from each of the two lines were chosen. Using (3) the homogeneous image coordinates of these two pairs of points (x_{Laser}), were transformed to the corresponding grid coordinate point (X_{plane}) of the plane by using the respective planar homography ($H_{\{V,H\}3x3}$) of the corresponding plane. Using (4) the homogeneous grid coordinate points were transformed to homogeneous point (X_{Laser}) in camera coordinate frame, world reference frame .

$$X_{plane_i}=H_{\{V,H\}3x3}^{-1}\cdot x_{Laser_i} \quad (3)$$

Where $H_{\{V,H\}3x3}^{-1}$ is the inverse of $H_{\{V,H\}3x3}$

$$X_{Laser_i}={}^{C}T_{\{V,H\}}\cdot X_{Hplane_i} \quad (4)$$

Where

$$X_{Hplane_i}=\begin{bmatrix} X_{plane(x)_i}/X_{plane(z)_i} \\ X_{plane(y)_i}/X_{plane(z)_i} \\ 0 \\ 1 \end{bmatrix}$$

A 3-D plane is defined by a 3-D point on the plane (m)

and the unit normal vector of the plane ($\vec{n}$) such that any 3-D point X on the plane will satisfy (5).

$$\vec{n}\cdot(X-m)=0 \quad (5)$$

Resolving for $\vec{n}$ we obtain (6).

$$\vec{n}=(\vec{v}_1\times\vec{v}_2)/\sin(\theta) \quad (6)$$

Where

$$\vec{v}_1=(X_{Laser1}-X_{Laser2})/\|(X_{Laser1}-X_{Laser2})\|$$
$$\vec{v}_2=(X_{Laser1}-X_{Laser3})/\|(X_{Laser1}-X_{Laser3})\|$$
$$\theta=\cos^{-1}(\vec{v}_1\cdot\vec{v}_2)$$

The corresponding point of the normal was obtained by (7).

$$m=\frac{\sum_{(i=1)}^{4} X_{Laser_i}}{4} \quad (7)$$

In the second method the estimation of the laser plane parameters was computed in 3-D space. This was carried out as follows: firstly all the detected laser points were transformed to 3D points in the camera frame using (3) and (4) as explained earlier in this section. Using a plane fitting algorithm a plane was estimated to fit the points. To obtain the best fitting plane through a 3-D georeferenced data, and thus estimate the plane parameters (m and $\vec{n}$), the Moment of Inertia Analysis (MIA) method[19][20] was used. MIA has the advantage of being able to provide the quantitative measure of the shape of the trace and also give a measure of the reliability of the data set. For more information about how to obtain the above measures refer to the paper by Fernandez [19].

The plane parameters (m and $\vec{n}$) of the best fitting plane was found as follows:

For N detected image locations in the 3-D camera reference frame, $X_{Laser_{1..N}}$ it was assumed that the best-fitting plane passes through the mean of the $X_{Laser_{1..N}}$ ($m=mean(X_{Laser_{1..N}})$). Hence the orientation matrix T was obtained as shown in (8).

$$T=\begin{Bmatrix} \sum(a_i^2) & \sum(a_ib_i) & \sum(a_ic_i) \\ \sum(b_ia_i) & \sum(b_i^2) & \sum(b_ic_i) \\ \sum(c_ia_i) & \sum(c_ib_i) & \sum(c_i^2) \end{Bmatrix} \quad (8)$$

Where

$$\begin{Bmatrix} a_i \\ b_i \\ c_i \end{Bmatrix}=\begin{Bmatrix} X_{Laser(x)_i}-m_x \\ X_{Laser(y)_i}-m_y \\ X_{Laser(z)_i}-m_z \end{Bmatrix} \quad (9)$$

For $i = 1..N$

The eigenvector corresponding to the smallest eigenvalue of the matrix T was taken as the normal $\vec{n}$ of the laser plane.

The performance of the two methods described above, of estimating the laser plane parameters, was evaluated as discussed below. POV-ray[11] is used to generate synthetic noise free images of perfect laser planes with known parameters for known camera intrinsic parameters (Appendix,

Table 1:
Laser plane pose estimation result of using the HT

	Plane parameters		Estimated (HT)		Error	
	Rotation	Translation				
Image	(r), degree	(t), unit	r	t	r	t
1	0.00	0.20	1.295	0.184	1.295	-0.016
2	0.00	-2.20	2.626	-2.187	2.626	0.013
3	10.00	0.00	9.884	0.000	-0.116	0.000
4	20.00	0.00	20.117	0.000	0.117	0.000
5	25.00	0.00	25.053	0.000	0.053	0.000
6	-25.00	0.00	-26.480	0.000	-1.480	0.000
Root Mean square(RMS) error:					0.548	0.003
Maximum Error:					2.626	-0.016

Table 2:
Laser plane pose estimation result of using Moment of Inertial.

	Plane parameters		Estimated (MIA)		Error	
	Rotation	Translation				
Image	(r), degree	(t), unit	r	t	r	t
1	0.00	0.20	0.012	0.183	0.012	-0.017
2	0.00	-2.20	0.074	-2.182	0.074	0.018
3	10.00	0.00	9.884	0.000	-0.116	0.000
4	20.00	0.00	20.005	0.000	0.005	0.000
5	25.00	0.00	25.079	0.000	0.079	0.000
6	-25.00	0.00	-25.046	0.000	-0.046	0.000
Root Mean square(RMS) error:					0.028	0.004
Maximum Error:					0.116	-0.017

Figure 8). The different laser plane images, of two pixel width, were generated by rotating the laser plane (r degree) around the Z-axis of the camera frame and then translating them to different locations with t units in the POV-ray unit system. The hough transform (HT) based method and the Moment of Inertia Analysis (MIA) based method were used to estimate the parameters of the generated planes. For the HT method the best fit line is found by stepping thorough one pixel and $\pi/180$ radian. The result of estimating the planes' parameters using the two different methods were shown in table 1 and table 2. It can be seen that the overall performance of the MIA method was better when compared to HT method.

4)Surface reconstruction of a scanned object

The surface of a 3-D object was reconstructed by estimating the coordinates of a cloud of 3-D points lying on the surface of the object. The 3-D coordinates of the points were estimated as explained below. The N number of 2-D laser points $q(x_{1..N}, y_{1..N})$ on the surface of the object were transformed to 3-D space as explained below.

From the camera pinhole projection model a point in an image will lie on a ray $\vec{r}_i(x,y,z)$,(11), which passes through the center of the camera and the point on the scanned object which formed the image [21]. Using this model the 3-D coordinates, $Q_i(x,y,z)$, of the laser points on the surface of the object could be resolved by finding the intersection of $\vec{r}_i$ with the laser plane (10). Thus a cloud of 3-D points, $Q_i(x,y,z)$, representing the surface of the scanned object was generated at the end of the 3-D reconstruction process

$$Q_i = k \cdot \vec{r}_i \tag{10}$$

Where

$$k = \frac{m_x n_x + m_y n_y + m_z n_z}{r_x n_x + r_y n_y + r_z n_z}$$

and

$$\vec{r}_i = E^{-1} \cdot \begin{bmatrix} q_i(x) & q_i(y) & 1 \end{bmatrix}^T \tag{11}$$

Where E^{-1} is the calibrated camera intrinsic parameters and T is the transpose operation.

III. Results and Discussion

Figure 4 shows the results of the 3-D surface reconstruction of a scanned white object having the shape of a staircase. The actual depth and height of each step was 10mm(+/-0.5mm) and at right angle (+/- 1 degree) to each other. The scale used in the system was 1:24.33 millimetre (which was the size of a black square on checker board, the calibration object). The accuracy of the scanning process was evaluated as explained below. A laser plane was aligned along the side of the object, to generate a contour as shown in Figure 5. The 3-D points were plotted (Figure 6) and the corresponding 3-D points (P1 to P7) were approximated. The distance and angle between the points were measured. The plane with the same orientation was translated by 5mm and the laser contour was extracted again. The process was repeated six times. The 3-D plots of all the laser contours were plotted (Figure 7). Each scan provided six measurements for the depth and height of the staircase and five measurements for the angle, *e.g.* the angle at location $P2$ produced by vector $P1-P2$ and $P2-P3$). The measurement results of the first laser contour (Figure 5) are shown in Table 3. Totally thirty six measurements for the depth and the height and thirty measurements for the angle were taken. The standard deviation of the total measured height and depth was 1.05mm. The standard deviation of the measured angle was 4.98 degree.

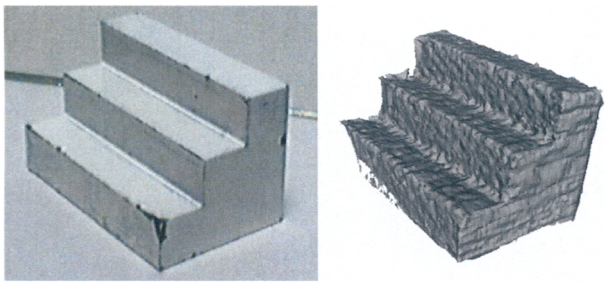

Figure 4: The 3-D object that was scanned (left); A staircase each step of 10mm depth and 10mm height and 90 degree, made with +/-0.5mm and +/-1 degree accuracy.

The 3-D surface reconstruction of the object (right) from a single view (right).

Conclusion

In this paper we have presented an implementation of a freehand laser scanner system. For the system, both hardware and software, off-the-shelf components were used. The result of the 3-D surface reconstruction was presented and the accuracy of the system was evaluated. The 3-D laser scanning system can be subsequently modified for different applications, for example the 3-D reconstruction of human anatomy and creating a 3-D profile to represent an object that needs to be tracked.

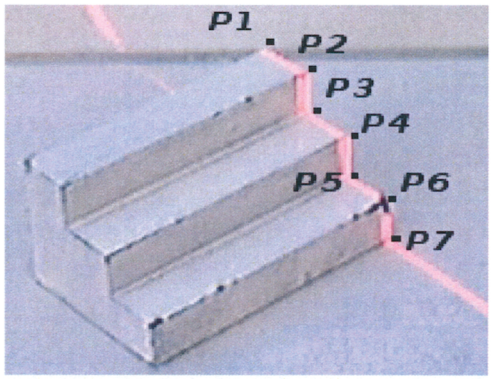

Figure 5: Intersection of the laser plane with the 3-D object. The original camera image is shown in the appendix (Figure 9)

Figure 6: 3-D plotting of laser points lying on the 3-D object.

Table 3:
The result of measurement for the laser points in Figure 6.

Distance between Points (mm)		Angle(degree)	
P1 and P2	11.19	At P2	89.20
P2 and P3	9.33	At P3	86.55
P3 and P4	11.18	At P4	85.54
P4 and P5	10.16	At P5	85.17
P5 and P6	10.88	At P6	87.90

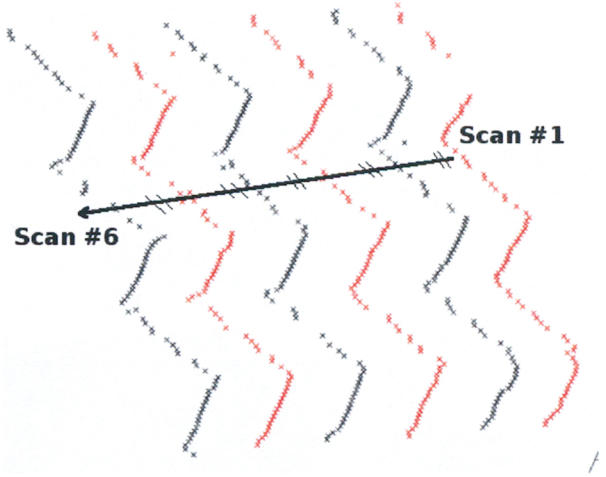

Figure 7: 3-D plots of the parallel scans.

APPENDIX

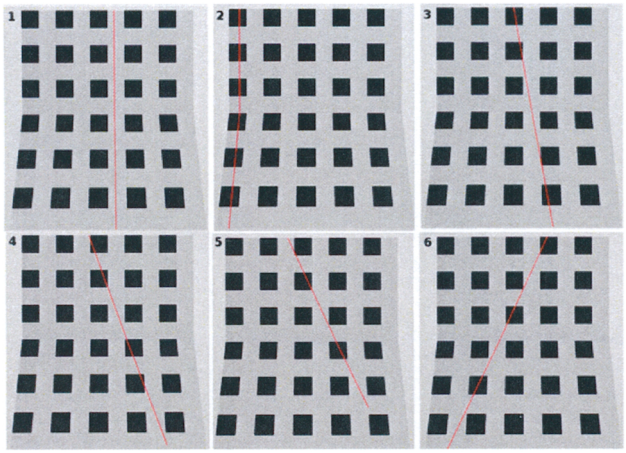

Figure 8: Six synthetic images generated by using POV-ray. Images are used to compare the performance of laser plane pose detection algorithms. The camera is fixed at POV-ray world origin and looking at z-axis direction. The vertical plane is perpendicular to the camera z-axis and the horizontal plane is rotated at x-axis by 20 degree. The width of laser plane is 0.02 unit (one unit is equivalent to 2 times the size of a black color square.

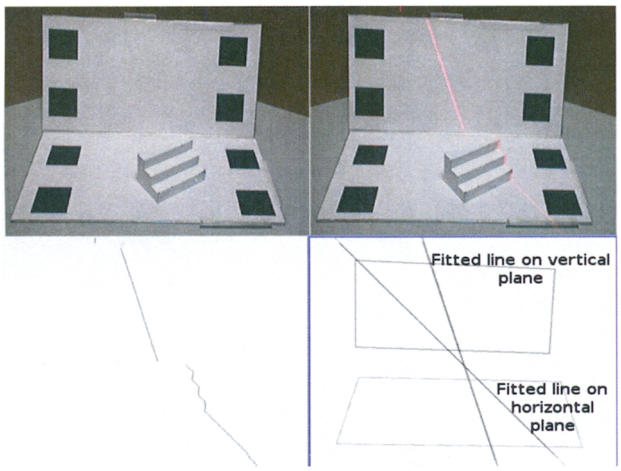

Figure 9: Camera captured images (top row): Scene image, Img_{bg} (top left); Scene image with laser line, Img_L (top right). Processed images (bottom row): Detected laser pixels using background subtraction method (bottom left); two corresponding lines obtained with HT line fitting algorithm (bottom right).

ACKNOWLEDGEMENT

The authors would like to thank Mr. Julien Faucher for developing the initial prototype (camera calibration, planar homography and corner detector) and also Mr. Arul N. Selvan and Mr. Jan Wedekind for their support. Kim Chuan Lim would also like to acknowledge UTeM, Malaysia for his scholarship award.

REFERENCES

[1] J.Y.Bouguet, "Visual methods for three-dimensional modeling", Ph.D. dissertation, California Institute of Technology, Pasadena, CA, USA, 1999.

[2] F. Isgro, F. Odone and A. Verri , "An Open System for 3D Data Acquisition from Multiple Sensor",Computer Architecture for Machine Perception, 2005. CAMP 2005, *Proceedings. Seventh International Workshop on* pp. 52-57

[3] G. J.Power, K.A. Xue, "Non-Linear Transform Technique for a Camera and Laser 3-D Scanner", Aerospace and Electronics Conference, 1995. NAECON 1995, *Proceedings of the IEEE 1995 National,* vol 2, pp 843

[4] Immersion, *3D Laser Scanner: Lightweight, Compact,Affordable*,Available: <http://www.immersion.com/digitizer/products/laser.php>, [Accessed: Aug 08 2008].

[5] Y.A.Vershinin, "3D Digital Surface Reconstruction Scanner for Medical Application", Signal and Image Processing, *Proceedings of the Fourth IASTED International Conference*, August 12-14,2002, Kaua'i, Hawaii, USA. pp 491-496

[6] H.Kawasaki,R.Furukawa, "Entire model acquisition system using handheld 3D digitizer", 3D Data Processing, Visualization and Transmission, 2004. 3DPVT 2004. *Proceedings. 2nd International Symposium on*,2004, pp.478-485.

[7] T.Pajdla, "Laser Plane Range Finder The Implementation at the CVL", Computer Vision Laboratory, Czech Technical University, Prague, 1995

[8] S. Winkelbach, S. Molkenstruck, and F.M. Wahl, "Low-Cost Laser Range Scanner and Fast Surface Registration Approach", Pattern Recognition (DAGM 2006), *Lecture Notes in Computer Science*,2006,vol. 4174,pp. 718-728.

[9] L.Zagorchev, and A. Goshtasby, "A paintbrush laser range scanner", *Computer Vision and Image Understanding*, Elsevier, 2006, vol. 101, pp. 65-86.

[10] J.Y.Bouguet, *Camera Calibration Toolbox for Matlab*, Available:<http://www.vision.caltech.edu/bouguetj/calib_doc/>, [Accessed: Aug 08 2008].

[11] POV-Ray, *POV-Ray - The Persistence of Vision Raytracer*, Available:<http://www.povray.org/>, [Accessed: Aug 08 2008].

[12] N. Amenta, S. Choi, and R.K. Kolluri, "The power crust", *Proceedings of the sixth ACM symposium on Solid modeling and applications*, 2001, pp. 249-266.

[13] P. Cignoni, *MeshLab*, Available: <http://meshlab.sourceforge.net/> [Accessed: Aug 08 2008]

[14] B.P. Amavasai, "A vision toolkit for real-time imaging", ERC Seminar, Sheffield Hallam University, 29 January 2003.

[15] M.K. Dalheimer, *Programming with Qt.* O'Reilly, 2002.

[16] Z. Zhang, "A Flexible New Technique for Camera Calibration", *IEEE Transactions on Pattern Analysis and Machine Intelligence*, 2000.

[17] R. Fisher and D. Naidu, "A Comparison of Algorithms for Sub-pixel Peak Detection", In *Proc. 1991 British Machine Vision Association Conf*, pages 217-225, 1991

[18] R.O. Duda, P.E. Hart, "Use of the Hough transformation to detect lines and curves in pictures", *Communications of the ACM*, Vol. 15, No. 1, pp. 11-15, 1972.

[19] O. Fernandez, "Obtaining a best fitting plane through 3D georeferenced data",*Journal of Structural Geology*, 2005,vol. 27, pp.855-858

[20] N.H. Woodcock, "Specification of fabric shapes using an eigenvalue method." *Geological Society of America Bulletin* 88, 1977, pp.1231-1236

[21] Y. Ma, *An Invitation to 3-D Vision.* Springer-Verlag, New York,U.S.A., 2004.

[22] J. Faucher, "Camera calibration and 3-D reconstruction", Master thesis, Sheffield Hallam University, U.K, 2006.

[23] O. Faugeras, "Three-Dimensional Computer Vision: A Geometric Viewpoint", Mit Press, 1993.